vehicles

Article

Improving the Efficiency of Electric Vehicles: Advancements in Hybrid Energy Storage Systems

Mostafa Farrag, Chun Sing Lai *, Mohamed Darwish and Gareth Taylor

Department of Electronic and Electrical Engineering, Brunel University London, London UB8 3PH, UK; mostafa.farrag@brunel.ac.uk (M.F.); mohamed.darwish@brunel.ac.uk (M.D.); gareth.taylor@brunel.ac.uk (G.T.)
* Correspondence: chunsing.lai@brunel.ac.uk

Abstract: Electric vehicles (EVs) encounter substantial obstacles in effectively managing energy, particularly when faced with varied driving circumstances and surrounding factors. This study aims to evaluate the performance of three different control systems in a fully operational hybrid energy storage system (HESS) installed in the Nissan Leaf. The objective is to improve the performance of EVs by focusing on optimising energy management in response to different global environmental and driving circumstances. This study utilises an analytical strategy by developing a distinct energy management system model using MATLAB/Simulink. This model is specifically designed for optimising the integration and control of batteries and supercapacitors (SCs) in a fully active HESS. This model mimics the performance of the controllers under three different driving cycles—Artemis rural, Artemis motorway, and US06. The findings demonstrate notable progress in managing the battery state of charge (SOC) and the system's responsiveness, especially when employing the radial basis function (RBF) controller. This study emphasises the capacity of HESSs to enhance the effectiveness and durability of EVs, therefore promoting wider acceptance and progress in electric transportation technology.

Keywords: electric vehicles; hybrid energy storage system; proportional-integral controller; model predictive control and radial basis function

Citation: Farrag, M.; Lai, C.S.; Darwish, M.; Taylor, G. Improving the Efficiency of Electric Vehicles: Advancements in Hybrid Energy Storage Systems. *Vehicles* **2024**, *6*, 1089–1113. https://doi.org/10.3390/vehicles6030052

Academic Editor: Yiqun Liu

Received: 14 May 2024
Revised: 19 June 2024
Accepted: 26 June 2024
Published: 28 June 2024

1. Introduction

Electric vehicles (EVs) have attracted considerable interest in the past decade owing to their capacity to replace traditional combustion engines (ICEs), recognised for their environmental impact. The United States witnessed the first wave of effort for developing an EV that is compatible with road transportation in as early as 1834 [1]. The shift towards EVs has been facilitated by advancements in storage technology, energy management systems, and motor efficiency. There are numerous advantages associated with the adoption of pure electric vehicles. These advantages encompass a simpler and more reliable infrastructure, reduced and more cost-effective maintenance, much lower transportation expenses—up to tenfold lower in comparison to traditional vehicles—as well as the instantaneous accessibility of complete power throughout the entire RPM spectrum. Furthermore, governments frequently promote the adoption of EVs by implementing tax reductions and grants, thus bolstering their economic feasibility.

While there are other innovations available, such as Plug-in Hybrid cars (PHEVs) and Fuel Cell Vehicles (FCVs), EVs exhibit extraordinary energy efficiency, which drastically impacts their performance. The results can be obtained from Table 1, displaying less energy dissipation, energy consumption, and higher efficiency rates than other types of vehicles. The assessment of energy dissipation using the 'Well-to-Wheel' (WTW) methodology, which considers the complete energy flow from gasoline extraction to power gearbox at the vehicle's wheels, further emphasises the efficiency benefits of pure EVs [2]. This thorough evaluation emphasises the decreased energy inefficiency of EVs in comparison to their hybrid and fuel cell counterparts.

In addition to the characteristics illustrated in Table 1, EVs demonstrate a potential for energy efficiency that is up to four times greater than ICEs, and their energy can be derived from sources of clean energy. This feature greatly alleviates the greenhouse effect and minimises air pollution, especially in urban areas. The positive environmental effects of EVs can immediately outweigh the emissions produced throughout the production process. Figure 1a depicts the current expansion in the market share of EVs [3]. It is necessary to tackle certain issues to facilitate the widespread adoption of EVs over ICE vehicles [4]. The problems can be classified into four primary categories, as depicted in Figure 1b [5]:

a. Practical: challenges encompass prolonged charging durations, a shortage of public rapid chargers, weighty batteries, and restricted vehicle self-sufficiency, exacerbated by undeveloped energy management systems.
b. Economic: the high expenses, elevated electricity bills resulting from rising demand, and limited profitability discourage widespread popularity.
c. Social: despite incentives, user concerns regarding the range and safety of the vehicle, as well as a reluctance to shift away from traditional vehicles, obstruct adoption.
d. Environmental: The sustainable utilisation of electric vehicles necessitates using clean sources of electricity and implementing effective recovery techniques for hazardous batteries. Additionally, it is crucial to tackle the consequences associated with the extraction of rare materials.

Table 1. Analysis of various vehicle technologies in terms of their impact on road operation [5].

Type	Energy Dissipation	Efficiency	Energy Consumption (kWh/km)
Gasoline	86%	14%	1.36
Diesel	80%	20%	0.95
Liquefied Petroleum Gas	84%	16%	1.19
Compressed Natural Gas	81%	19%	1.00
PHEV	55%	45%	0.42
FCV	78%	22%	0.87
Battery/EV	33%	67%	0.28

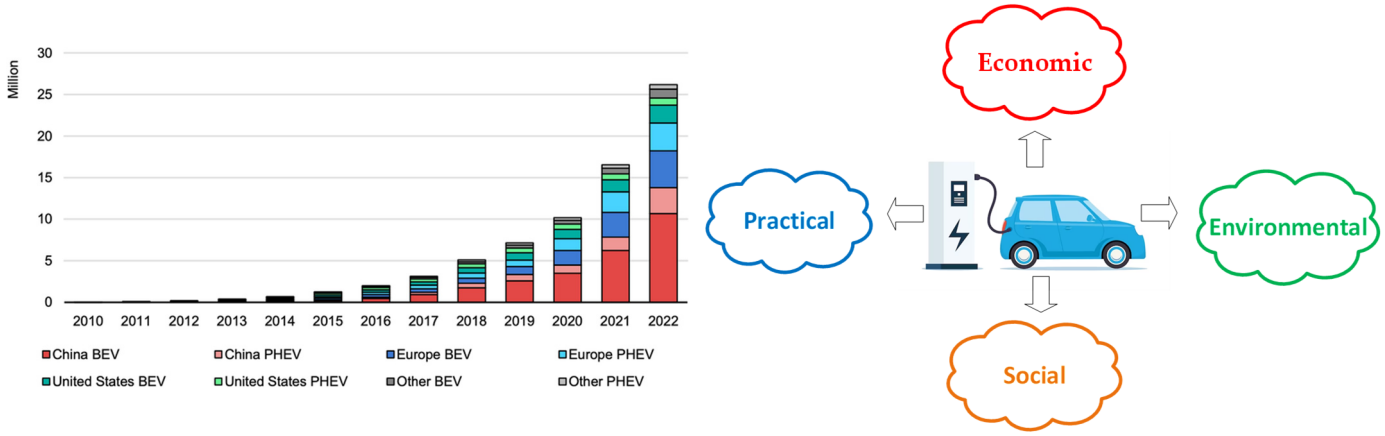

(**a**) (**b**)

Figure 1. Composite overview: (**a**) global electric vehicle market growth [3]; (**b**) key factors influencing the adoption of electric vehicles [5].

The widespread use of EVs in transportation leads to a significant reduction in energy wastage, despite the ongoing presence of reliability and effectiveness problems in existing storage systems. Over time, electrochemical batteries age and experience a reduction in

capacity, which requires them to be replaced. In order to tackle this issue, recent studies have investigated a hybrid energy storage system (HESS) that integrates both batteries and supercapacitors (SCs). SCs, characterised by their high power density (Wh/kg) but low energy density (W/kg), play a crucial role in HESSs. These systems combine the advantages of SCs with batteries. While batteries can sustain high cycling numbers, they are unsuitable for high discharge rates. This is a considerable benefit of incorporating SCs with batteries in a HESS. The performance and lifespan of the energy storage system in EVs are improved by this combination, which capitalises on the high power density of SCs and the high energy density of batteries. Furthermore, the integration of an HESS not only improves the response speed and improves the system's lifespan, but also reduces the total size and expenses, which boosts the system's reliability and balance. This combination significantly reduces the constraints of utilising a single energy storage method, thereby offering a more efficient and durable solution for EVs [6].

An important obstacle in HESS design involves analysing the configuration of the SC and battery with regard to the DC (Direct Current) bus. Various configurations for battery–SC interconnections have been investigated and explored, each exhibiting distinct merits and drawbacks. Several studies in the literature have strived to develop battery–SC HESSs for EVs, adopting different configurations to connect the battery and the SC [7–10]. Figure 2 depicts various configurations of HESSs [11]. The fully active HESS is one of the most widely used topologies, as represented in Figure 2d. A broad range of energy management strategies have been proposed and have attracted significant interest among EV communities' societies. This setup establishes a connection between both components and the DC bus using bidirectional DC–DC converters, providing notable benefits. This configuration enables an effective energy allocation and a quick adaptation to power requirements, enhancing the overall efficiency and durability of the electric vehicle's energy storage system. By capitalising on the high power density of supercapacitors and the high energy density of batteries, the fully active HESS optimises energy efficiency, guaranteeing dependable and consistent operation in a variety of driving scenarios.

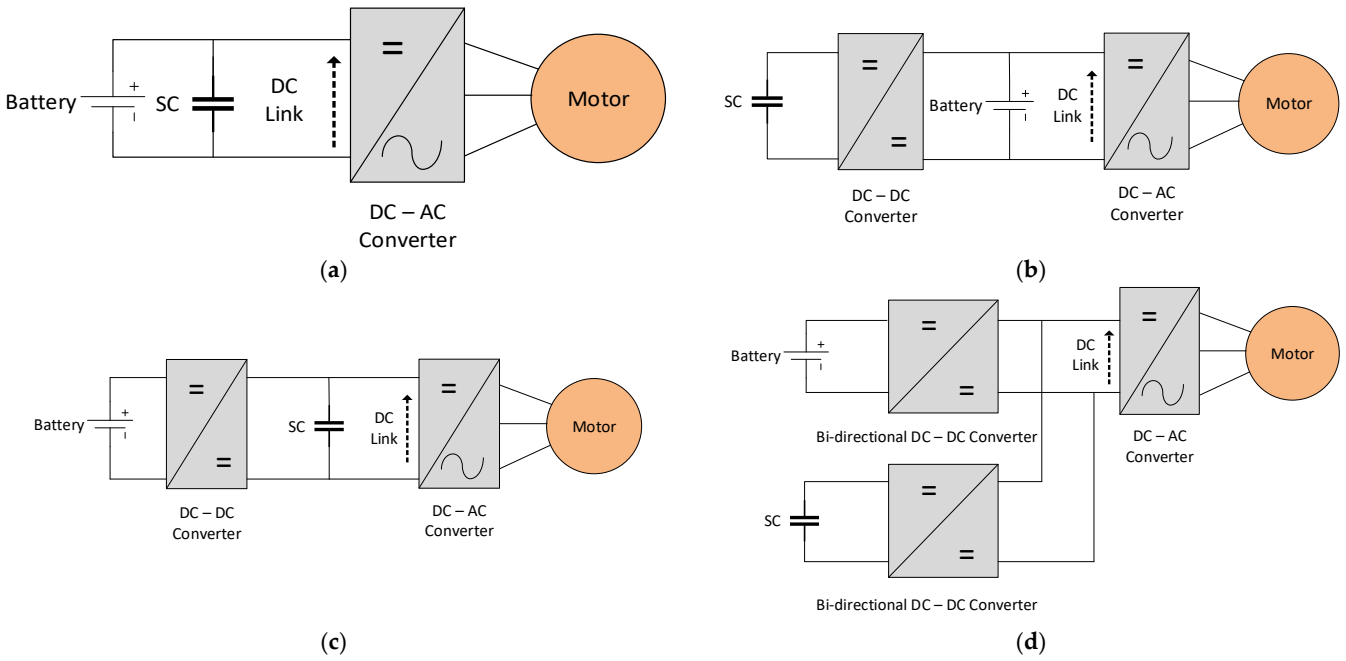

Figure 2. HESS configurations: (**a**) passive parallel, (**b**) controlled SC, (**c**) controlled battery, (**d**) fully active.

1.1. Related Work

In determining how efficient HESSs are in managing the stress posed by charge and discharge cycles on energy storage systems, the implementation of an appropriate control strategy for the energy management strategy is crucial. Rule-based approaches and optimisation algorithm-driven approaches are the two primary classifications of these methodologies.

Rule-based controllers are commonly referred to as deterministic rules and fuzzy logic control. The authors of [12] carried out a study to allocate the power demand between the SC and battery energy sources using several techniques, such as the PI approach, the external energy maximisation strategy, and the equivalent consumption reduction. Consequently, the SC regulates the DC bus voltage, which exhibits rapid dynamics, while the battery maintains the load power. In [13], the classical proportional-integral-derivative (PID) regulator is utilised in Battery/SC HESSs for EVs due to its proven ease and dependability. However, this type of regulator can suffer significant degradation when faced with changing operating conditions, primarily due to issues related to local linearisation. In [14], the author developed a fuzzy logic controller to regulate the power distribution between the battery and the SC. The controller's input consisted of the overall vehicle load demand and the state of charge (SOC) of the SC and the battery. The simulated vehicle's control strategy was implemented using the ADVISOR platform. A fuzzy logic controller was utilised in [15] to regulate the HESS for EVs. The objective of the regulator was to allocate the power load between the battery and the SC, to maintain the voltage of the DC bus, and to monitor the SOC of the SC. The findings demonstrated that the recommended controller prolonged the longevity of the battery by consistently providing the load energy from the battery during stable periods and from the supercapacitor during transient periods. A fuzzy rule-based energy management system has been developed in study [16]. This was developed to optimise the SOC of both the SC and the battery. Moreover, the controller utilises the real-time speed of the vehicle as an input to optimise the power distribution of the energy management system. Deterministic and fuzzy logic rule approaches can greatly improve energy efficiency; however, they have limitations, such as not being able to quickly adjust to new situations, not being able to scale with complicated structures, and prioritising practical solutions over optimal ones [17].

Optimisation-based approaches in the energy management of HESSs in EVs utilise past or projected driving data. These methods tackle both local and global optimisation difficulties by using prior driving cycle data to find the most efficient allocation of power across energy storage devices. The optimisation of HESSs for EVs has been thoroughly investigated to improve the lifetime of batteries and to increase the overall efficiency of the system. Adaptive filter-based strategies have proven effective in enhancing HESSs in EVs. A study by the authors of [18] utilised an artificial potential field (APF) in conjunction with a feed-forward compensator to dynamically regulate power allocation. This method decreases battery degradation and enhances system effectiveness by avoiding excessive charging and eliminating changes in the DC-link voltage. In [19], the author proposed an adaptive power split approach by employing dynamic Fourier spectrum analysis. This technique optimises power allocation according to current load requirements, enhancing power equilibrium and minimising battery degradation. Both research studies demonstrate the efficacy of adaptive filters in enhancing battery performance and prolonging the lifespan of energy storage components in HESSs for EVs [18,19]. Advanced control techniques, such as dynamic programming (DP), have also been pivotal in optimising HESS configurations and control methods. A study by the authors of [20] utilised a DP technique to optimise both the configuration of the HESS and the control techniques. This approach effectively reduced battery degradation by lowering the capacity rate of the discharge–charge current. Another study was carried out to create a power management strategy for PHEVs [21]. This strategy considered battery ageing mechanisms and variations in state-of-health. The study showed that incorporated optimisation approaches can effectively improve battery longevity and system performance in different driving conditions. These studies highlight the essential importance of advanced control techniques and dynamic programming in attaining sustain-

able and efficient energy management in EVs [20,21]. Incorporating neural networks and multi-objective optimisation techniques has yielded substantial improvements in energy management strategies. A study by the authors of [22] proposed a supervisory energy management technique that utilised DP and neural networks. This strategy resulted in a 60% increase in battery life and significant enhancements in energy efficiency. Similarly, another study adopted multi-objective optimisation and random forests to reach a nearly ideal performance, effectively maintaining a balance between system costs and battery lifespan [23]. These studies provide evidence of the effectiveness of integrating DP using real-time adaptive approaches [22,23]. Evolutionary algorithms have been beneficial for optimising HESSs. A study by the authors of [24] utilised a multi-objective evolutionary algorithm to enhance the performance and lifespan of HESSs in microgrids. They achieved notable advancements by considering cost, performance, and lifetime aspects in a balanced manner. In addition to this, another study addressed light rail vehicles using evolutionary algorithms to achieve multi-objective optimisation [25]. The results showed significant cost savings and improved operational efficiency in areas without overhead wires. These studies emphasise the crucial importance of advanced optimisation techniques in creating cost-efficient and reliable HESS solutions for dynamic transportation and microgrid applications [24,25]. Recent developments have highlighted the potential of sophisticated reinforcement learning algorithms in energy management systems for EVs with HESSs. A study by the authors of [26] presented an energy management system based on a soft actor–critic (SAC) approach. This system incorporated DP knowledge and parallel computing to improve control performance and training efficiency. As a result, it achieved notable reductions in energy loss and demonstrated an enhanced adaptability compared to conventional deep Q-network (DQN) and deep deterministic policy gradient (DDPG) methods. In addition to this, in [27], the author introduced an incentive learning-based energy management system for EVs that utilised battery–supercapacitor technology. The primary focus of this system was to reduce battery capacity and power loss. This approach integrated a system of rewards and procedures for initial training, resulting in enhanced speed and flexibility in learning across different driving scenarios. As a result, it achieved significant cost savings compared to current deep reinforcement learning methods. These studies demonstrate the potential of advanced reinforcement learning methods in optimising energy management systems for EVs that feature HESSs. Model predictive control (MPC) techniques offer remarkable accuracy and the ability to generate near-optimal future projections and responses. In [28], the author proposed a multi-horizon MPC approach for HEVs, optimising power allocation between the battery and supercapacitor, resulting in a 4.2% reduction in battery deterioration and improved efficiency. Despite the high accuracy of MPC, its performance heavily depends on the model of the controlled system. Khil et al. implemented the MPC technique using MATLAB Simulink and tested it on the dSPACE platform for HESSs [29], dynamically estimating reference currents for DC-link voltage control and reducing battery discharge rates. Chen et al. introduced a speed detection approach based on long short-term memory (LSTM) to forecast driving cycles, using this in an MPC approach to minimise battery energy loss [30]. Combining simulation and hardware in the loop, this study verified the performance of the energy management system, showing a 15.3% reduction in battery energy loss using MPC [30]. Those extensive studies demonstrate the significant progress and potential of various optimisation methods in improving the efficiency and durability of HESSs in EVs.

1.2. Main Contribuiton

The primary objective of this work is the development of an innovative energy management approach specifically designed for fully active HESSs in EVs. This technology employs advanced control systems to optimise the integration of SCs into traditional battery systems, resulting in a substantial increase in the operational efficiency of EVs under different environmental driving situations.

The rest of this paper is organised as follows: Section 2 presents the system and modelling, where it provides an overview and analysis of the system being studied. Section 3 outlines the chosen energy management control methodology and compares its performance against other methods. Also, it highlights how the chosen control technique improves system performance, saves energy, and aligns with the overall operational objectives of the system. Section 4 presents and discusses the results when applying three control strategies in EV HESSs using MATLAB/Simulink. Finally, the paper is concluded in Section 5.

2. Summary of the System and Modelling

This research investigates an EV that is propelled using a fully active HESS, which consists of a SC and a battery. This typical HESS configuration is illustrated in Figure 2d. The DC bus operates in parallel with the SC and battery banks through two-quadrant DC–DC converters. By adopting this particular configuration, the battery can effectively sustain the DC bus voltage at the appropriate level. Furthermore, it enables the HESS to interchange power in both directions, allowing the vehicle to recharge either the battery or SC during regenerative braking phases. It also facilitates the battery's power transfer by authorising it to charge the SC and recharge it. To determine how to develop the power flow controller, it is necessary to study the vehicle dynamics and the features of the SC, assuming that the battery is appropriately sized to cover a specific range. The subsequent two subsections provide a comprehensive explanation of the modelling process for the EV and the HESS.

2.1. Vehicle Model

The Nissan Leaf has been chosen as the proposed vehicle for this study, and its specifications are outlined in Table 2. The primary factors that affect the dynamics of a vehicle include aerodynamic force (F_{aero}), rolling force (F_{roll}), grading force (F_{grad}), and inertial force (F_{acc}). Each of these forces is an essential element in conducting a thorough examination of the vehicle's performance. These forces are integral to developing a reliable model that predicts the vehicle's power and energy consumption based on different driving scenarios, as illustrated in Figure 3. This comprehensive modelling is the first step in optimising the energy efficiency of the vehicle's drivetrain. Therefore, in this study, the grading force had been eliminated from the analysis, as it had a minimal effect on the main objective of examining driving resistance and power demands. This exclusion guarantees a more concentrated and effective evaluation of the vehicle's performance in suitable situations without introducing unneeded sophistication. Equation (1) is used to determine the total force on a vehicle [31].

$$F_{Total} = F_{aero} + F_{roll} + F_{grad} + F_{acc} \tag{1}$$

While in motion, a vehicle is exposed to a variety of different forces, one of which is aerodynamic drag. This force arises from the contact between the inbound and outgoing airflow. The determination of aerodynamic force can be achieved using Equation (2) [31].

$$F_{aero} = 0.5\,\rho\,C_d\,A_f\,v^2 \tag{2}$$

where ρ is air density, C_d represents the drag coefficient, A_f represents the frontal area of the vehicle, and v denotes velocity. The main cause of rolling resistance is the interaction between the road surface and the tyre. Both the friction of ball bearings and the power transmission system are factors that contribute to the rolling resistance. Rolling resistance increases in direct correlation with the mass of the vehicle. Equation (3) represents the force of horizontal road rolling resistance [31].

$$F_{roll} = C_{rr}\,m\,g \tag{3}$$

where C_{rr} is the coefficient of rolling resistance, m represents the mass of the vehicle in kilogrammes, and g represents the acceleration due to gravity in metres per second. Equations (4) and (5) are employed for calculating the gradient force and acceleration force.

$$F_{grad} = m\ g \sin\ (\theta) \tag{4}$$

$$F_{acc} = m\ a \tag{5}$$

where a represents the acceleration. The power required for an EV can be determined and expressed using Equation (6).

$$P_{Req} = F_{Total} * v \tag{6}$$

Table 2. Specifications for EV, battery, and SC modules [32,33].

Module	Parameter	Value	Unit
EV	A_f	2.14	m^2
	C_d	0.28	-
	C_{rr}	0.01	-
	g	9.81	m/s^2
	m	1567	kg
Battery	Nominal Pack Voltage	360	Volts
	Nominal Pack Capacity	24	kWh
	Number of Cells	192	-
	Parallel Number	2	-
	Nominal Cell Voltage	3.75	Volts
	Cell Nominal Capacity	64	Ah
SC	Maxwell BMO3000	-	-
	Nominal Pack Voltage	24	Volts
	Nominal Pack Capacity	85	Faraday
	Number of Cells	89	-
	Parallel Number	1	-
	Nominal Cell Voltage	2.7	Volts
	Cell Nominal Capacity	3000	Faraday

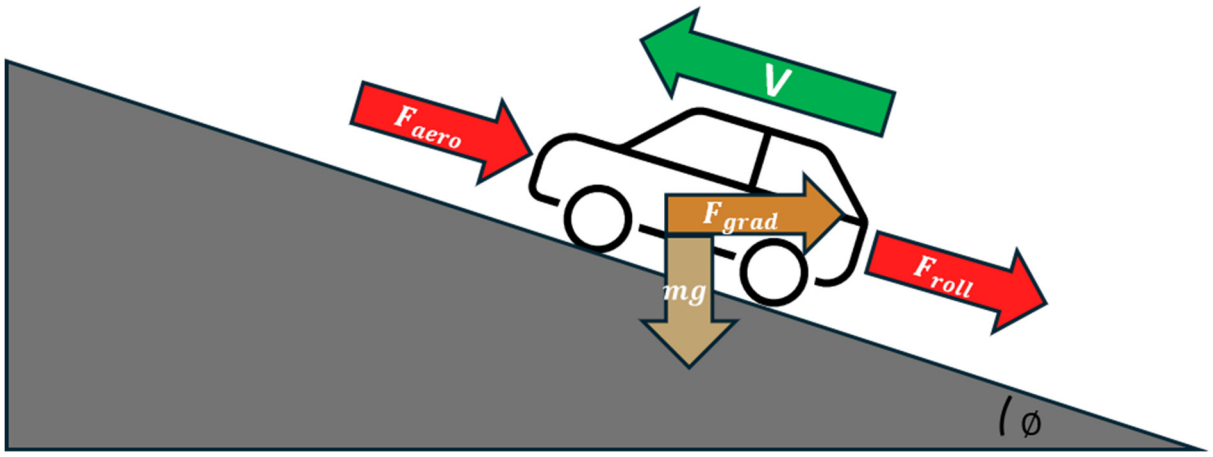

Figure 3. Vehicle forces.

2.2. Battery Model

The battery model depicted in Figure 4 has two integral equations to govern the charging and discharging operations, effectively capturing the operational dynamics of a

lithium-ion battery. Equation (7), which is crucial to the functioning and is illustrated in the selector switch mechanism Sel, is expressed as:

$$\frac{Exp\ (s)}{Sel\ (s)} = \frac{A}{\left(\frac{1}{B} * i(t) * s + 1\right)} \tag{7}$$

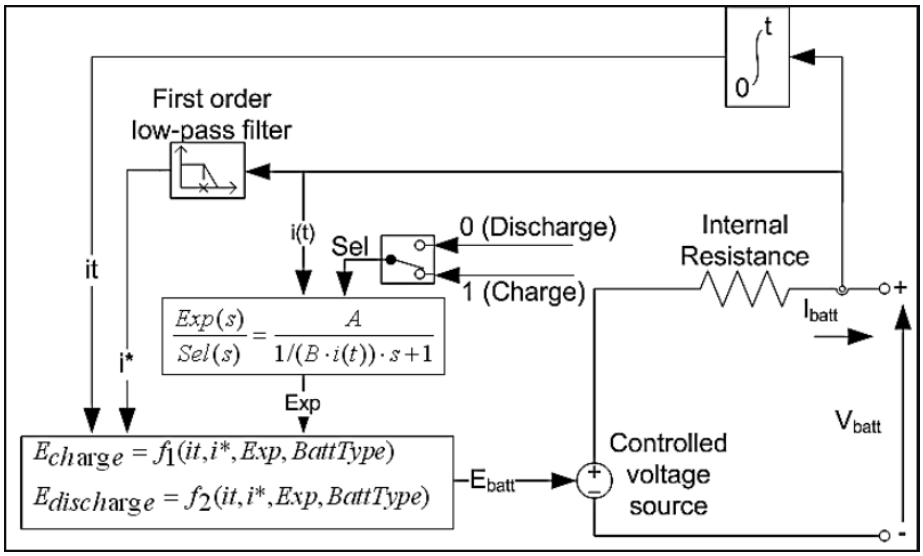

Figure 4. Battery equivalent circuit [34].

The above formula utilises an exponential smoothing $Exp\ (s)$ function to adjust the current $i(t)$, ensuring the system exhibits a seamless and progressive response to variations in load and charging circumstances. This equation is generated from the battery model and is designed to maintain efficiency and longevity by preventing sudden changes in current. This smoothing process provides an interaction between power demand, battery energy degradation, and Equation (7), which helps regulate the battery's reaction to power needs. The two constants A and B, combined with the variable s (from the Laplace transform domain) and the current $i(t)$, adjust the impact of the input current dynamically. This adjustment is carried out to match the operational mode determined using the $Sel\ (s)$ switch.

The model also includes a set of equations referred to as Equations (8) and (9), which are used to describe both the charging and discharging situations.

$$E_{charge} = f_1\ (it, i^*, Exp.BattType) \tag{8}$$

$$E_{discharge} = f_2(it,\ i^*,\ Exp.\ BattType) \tag{9}$$

Equations (8) and (9) play a crucial role in determining the amount of energy needed for charging and discharging by taking into consideration many variables, including the actual current (it), the filtered current (i^*), the exponential smoothing factor (Exp), and the battery type ($BattType$). By including these parameters, the equations play a crucial role in enabling the battery management system to accurately regulate energy distribution, thus improving efficiency and prolonging the battery's lifespan under different operational circumstances. The precise derivation and proper integration of these mathematical equations with the battery model's elements are crucial for efficiently controlling energy flows, as depicted in the battery model schematic.

2.3. SC Model

The SC model, depicted in Figure 5 presents a schematic representation of the equivalent circuit of an SC, wherein a controlled voltage source is connected to a cell featuring

an internal resistance. Two essential mathematical equations that are fundamental to comprehending the operational behaviour of the system are also depicted in the schematic. Equation (10) describes the total current i.

$$i = i_{sc} * (1 - u(t)) + i_{self_{dis}} * u(t) \tag{10}$$

where i_{sc} is the short circuit current, $i_{self_{dis}}$ is the self-discharge current, and $u(t)$ is the unit step function that controls the transition between normal operation and self-discharge. This configuration offers a comprehensive examination of how a cell reacts to different operational situations, encompassing the impact of internal chemical processes and external circuit parameters on the flow of electric current.

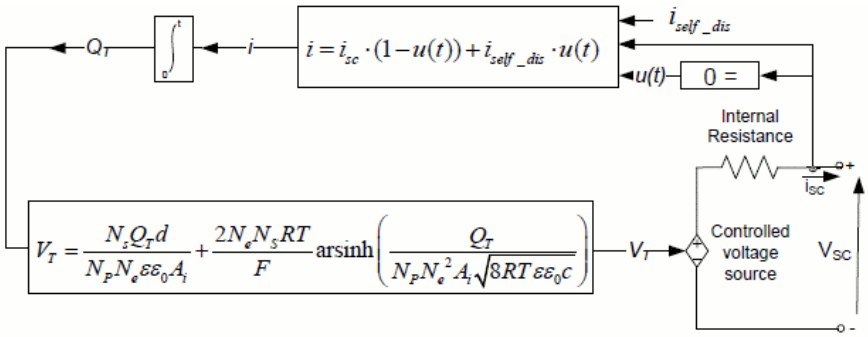

Figure 5. SC equivalent circuit [34].

The floating potential V_T, which is the potential when the cell is not supplying current to an external load, can be determined using Equation (11).

$$V_T = \frac{N_s \ Q_T \ d}{N_p \ N_e \ \in \in_0 \ A_i} + \frac{2 \ N_e \ N_s \ R \ T}{F} \ arsinh \left(\frac{Q_T}{N_p \ {N_e}^2 \ A_i \ \sqrt{8RT \ \in \in_0 \ c}} \right) \tag{11}$$

where N_s and N_p are the number of series and parallel connections of the cells, Q_T is the electric charge (C), d is the molecular radius, N_e is the number of layers of electrodes, $\in$ and $\in_0$ are the permittivity of material and free space, A_i is the interfacial area between electrodes and electrolyte (m^2), N_e is the number of layers of electrodes, R is the ideal gas constant, T is the operating temperature (K), F is the Faraday constant, and c is the molar concentration (mol/m^3).

Equations (10) and (11) above are crucial for precisely predicting the performance characteristics of electrochemical cells. They are particularly valuable in applications that need in-depth investigation of power distribution and storage behaviours under different electrical loads and situations. This knowledge is crucial for optimising battery management systems, improving reliability, and prolonging the lifespan of battery-powered equipment.

3. Controller Design

An effective controller is vital for solving the issues of optimising energy flows within an HESS to enhance the dynamic response and extend the battery life in EVs. The regulator has to carefully manage power distribution among the battery and SC to protect the battery from sudden power changes and to improve vehicle handling and passenger comfort. Figure 6 illustrates the structure of the system used in this study. This section provides an overview of the design concerns for three specific types of controllers—PI, MPC, and RBF.

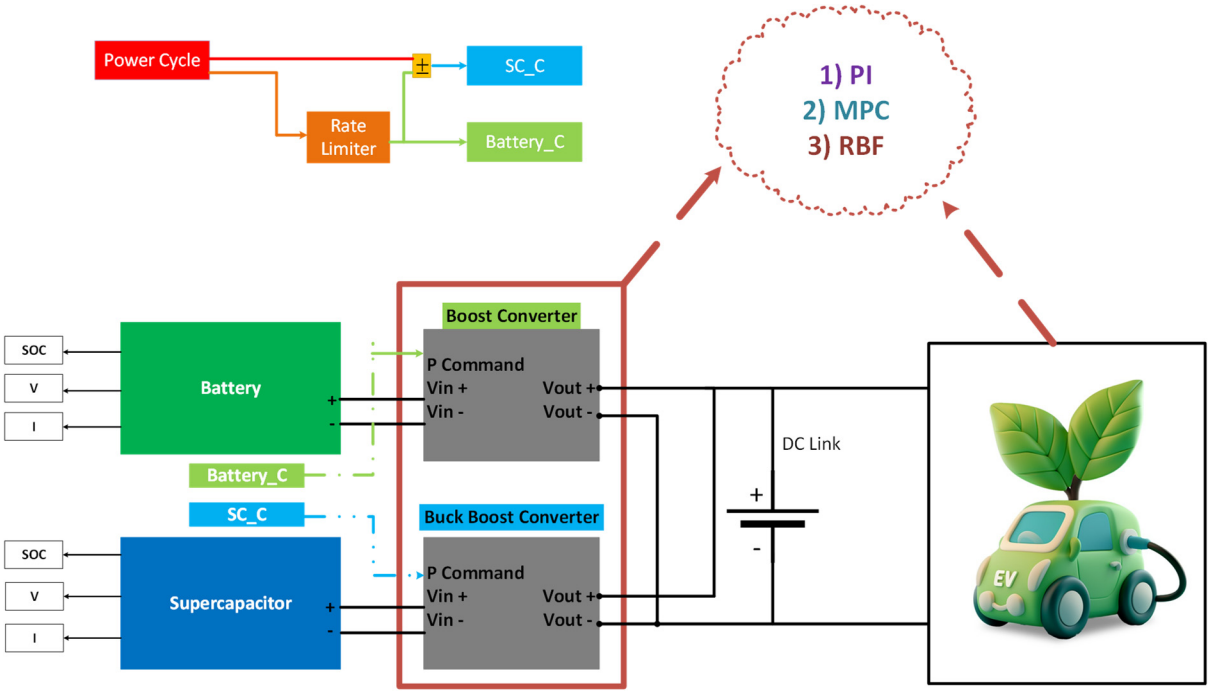

Figure 6. Construction of the proposed system.

3.1. PI Controller

The PI regulator is used for optimising the power allocation among batteries and SCs, assuring the system operates efficiently. The purpose of the regulator is to reduce the difference between the desired reference value and the actual result, which is expressed in Equation (12).

$$e(t) = r(t) - y(t) \tag{12}$$

where $r(t)$ represents the setpoint and $y(t)$ represents the actual measurement. Here, $e(t)$ is the difference between the desired reference value and the actual measured value. The regulator responds by adjusting the control action, which is expressed in Equation (13).

$$u(t) = K_p * e(t) + K_i \int e(t)dt \tag{13}$$

where K_p and K_i represent the proportional and integral gains, respectively. These gains serve as essentials for guaranteeing the stability and precision of the system. The output $u(t)$ is used to control the pulse-width modulation (PWM) signal, which controls the switching operations of the converter in the HESS. This adjustment facilitates the adaptation of the charge and discharge cycles following the changing power demands. The controller effectively maintains the desired performance levels, thereby optimising energy consumption and response times, which are critical in EV applications, due to the system's continuous feedback.

3.2. MPC

The MPC approach is considered to be one of the best control strategies to effectively regulate the power conversion in an HESS utilised in an EV, specifically concentrating on DC–DC converters. The MPC approach is specifically developed to optimise a cost function to forecast future system states by assessing the future state of the inductor current ($I_{L,k+1}$), as delineated in Equation (14).

$$I_{L,k+1} = \left(\frac{t_s}{L}\right) * (V_{in} - I_L * R_L - V_{out} * (1 - State_n)) + I_L \tag{14}$$

where t_s is the sampling time, L is the inductance, R_L is the load resistance, $State_n$ indicates the converter mode (Buck or Buck-Boost), V_{in} is the input voltage, V_{out} is the output voltage, and I_L is the inductor current. $State_n$ alternates between the Buck and Buck-Boost modes depend on the voltage needs of the DC bus in comparison with the input voltage. To systematise this procedure, Equation (15) represents an inequality condition that can be used to dynamically ascertain the suitable state of the converter, guaranteeing the most efficient voltage adjustment, whether it be a raise or decrease, based on the requirements of the system.

$$State_n = \begin{cases} \text{'Buck'} & \begin{pmatrix} if\ V_{in} > V_{out} \\ if\ V_{in} \leq V_{out} \end{pmatrix} \\ \text{'Buck} - \text{Boost'} \end{cases} \tag{15}$$

The above equation guarantees that the converter mode is chosen to either increase or decrease the voltage according to current power demands. More precisely, when the input voltage (V_{in}) from the energy storage is higher than what the output load requires, the Buck mode is employed to decrease the voltage. On the other hand, if the output load needs a voltage higher than what is stored, the Buck-Boost mode is engaged to raise the voltage. This technique enhances the energy efficiency of the system by altering the voltage levels to meet the individual requirements at any given moment, hence reducing energy wastage and improving the overall performance of the system.

The cost function is optimised using the MPC outline, as is expressed in Equation (16).

$$J = \left| I_{Lref} - I_{L,k} \right| + w_f \ * \ | \ State_n - State_{old}| \tag{16}$$

where variables I_{Lref}, $I_{L,k}$, w_f, $State_n$, and $State_{old}$ represent the reference inductor current, predicted inductor current at step k, weighting factor, and current and previous states of the converter, respectively. w_f imposes a penalty on the cost involved with transitioning between states. The MPC algorithm assesses possible future states by computing the cost associated with each state, considering the deviations from the current reference state and the cost of transitioning between states. It then chooses the control action that leads to the lowest overall cost. This optimisation guarantees effective power management and minimises energy wastage inside the system.

3.3. Radial Basis Fucntion Controller

The radial basis function (RBF) controller approach is considered as the most effective controller within HESSs for EVs. The RBF controller enhances energy management by utilising a Gaussian activation function, which is expressed in Equation (17):

$$\Phi(x, \mu, \sigma) = e^{-(|\frac{x-\mu}{\sigma}|)^2} \tag{17}$$

where variables x, μ, and σ represent the input, the centre, and the spread. The function plays a vital part in determining the controller's response to changes in input, effectively modifying the system's behaviour to minimise errors and enhance reliability.

The weight (W), centre (μ), and spread (σ) parameters in the RBF are adjusted using the gradient descent technique. This approach improves these parameters by using the error obtained from the system's output, as shown in Figure 7. The weight update rule is expressed in Equation (18).

$$\Delta W = \lambda_w \ E\Phi(x, \mu, \sigma) \tag{18}$$

where variables ΔW, λ_w, E, and $\Phi(x, \mu, \sigma)$ represent the change in weight, the learning rate, the error, and the Gaussian activation function. This update is essential for fine-tuning the impact of the input features on the network's output. Equation (19) expresses the updated weight, guaranteeing that the system adjusts gradually.

$$W_k = \lambda_w E \varnothing_k(x, \mu, \sigma) + W_{k-1} \tag{19}$$

μ is adjusted using the formula shown in Equation (20).

$$\Delta\mu = \lambda_\mu WE \frac{(x-\mu)}{\sigma^2}\Phi(x,\mu,\sigma) \tag{20}$$

where $(x-\mu)$ represents the distance between the data point and the centre. This formula modifies the midpoint of the Gaussian activation function, enabling the function to maintain its responsiveness to the input data near the updated average. It is essential to update μ, in order to ensure that the Gaussian distribution appropriately represents the most significant data points. This adjustment maintains the precision of the model when handling various inputs, and strengthens the performance and dependability of the control system by enhancing its capacity to adjust to new conditions. The updated centre is determined using Equation (21).

$$\lambda_\mu WE \frac{(x-\mu)}{\sigma^2}\Phi(x,\mu,\sigma) + \mu_{k-1} \tag{21}$$

σ represents the width of the Gaussian bell curve, and can be obtained using Equation (22).

$$\Delta\sigma = \lambda_\sigma WE \frac{(x-\mu)^2}{\sigma^3}\Phi(x,\mu,\sigma) \tag{22}$$

The update rule plays a crucial role in regulating the responsiveness of the output to variations in the input. This enables the model to improve its ability to make generalisations or concentrate more specifically based on the specific driving conditions. Equation (23) expresses the new spread.

$$\sigma_k = \lambda_\sigma WE \frac{(x-\mu)^2}{\sigma^3}\Phi(x,\mu,\sigma) + \sigma_{k-1} \tag{23}$$

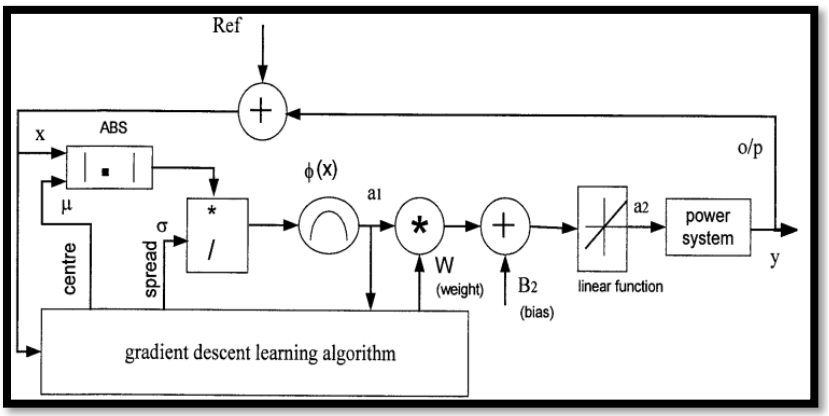

Figure 7. RBF controller schematic with gradient descent parameter optimisation.

For this work, the RBF performs a crucial role in optimising the operation of the DC–DC converter, which is essential for regulating the energy flow between batteries and SCs. The inputs of this controller include voltage levels (input and output), current measurements, and error signals (W, μ, and σ). The outputs are control commands for converter settings and parameter adjustments. The control commands executed using the RBF controller assure a flawless alignment between the power sourced from the battery or SC and the power produced from the converter side. Ensuring synchronisation is essential for preserving the effectiveness and steadiness of the energy transfer in the HESS, hence improving the overall efficiency of the EV. Furthermore, the adjustments made to the RBF controller to improve its adaptability and efficiency for this particular use have been discussed. These tasks involve enhancing the learning rate and adjusting the controller parameters to more accurately align with the characteristics of the electric vehicle's energy components. These adjustments guarantee that the RBF controller adequately tackles the

distinct obstacles presented by the EV environment, thereby enhancing both performance and energy efficiency.

The RBF controller utilises these methods to dynamically adjust its parameters, hence optimising the control approach for real-time energy management. The controller's capacity to continuously adjust these settings depending on the system's feedback loop makes it very efficient in handling the intricate dynamics of EVs, hence improving vehicle responsiveness. This adaptive mechanism guarantees that the EV functions at its best in various driving situations, utilising the maximum capabilities of its energy storage system.

3.4. Comparative Analysis of Control Strategies

To summarise, the PI controller offers simplicity and robustness for predictable situations, whereas MPC is particularly effective in optimising complicated systems by predicting future states. On the other hand, the RBF controller provides great precision in dynamic and unexpected contexts. By integrating various controllers, the unique advantages of each one are utilised to achieve optimal performance and reliability. Table 3 illustrates an overview of control strategy performance in EVs.

Table 3. Overview of control strategy performance in EVS.

Type	Key Findings	Merits	Demerits	Ref
PI	Proposed controller boosts EVs with HESS operating efficiency, energy efficiency, and stability.	• Simple, stable performance.	• Adequate dynamic response; • Nonlinearities present a challenge.	[35]
	Proposed controller improves fuel cell system performance and reliability for automotive applications, according to the research.			[36]
	Highlights how the proposed controller improves hybrid EV power system efficiency and stability.			[37]
MPC	Energy flow between storage components is dynamically adjusted based on the battery's SOC to improve energy efficiency and battery life.	• Effectively manages constraints • Predicts future states	• High computational burden • Implementation complexity	[38]
	MPC improves hybrid system efficiency and performance by dynamically modifying control actions based on vehicle mass estimates, according to the study.			[39]
	Demonstrates that recognising driving patterns improves MPC systems' prediction accuracy and energy management efficiency			[40]
RBF	Simulations show improved transition smoothness and system robustness during mode transitions.	• Highly proficient at managing nonlinearities • Demonstrates exceptional adaptability with learning mechanisms	• Necessitates a significant amount of training data • Carries the risk of overfitting, which can be mitigated with appropriate tuning	[41]
	Research shows that adaptive strategies enhance fuel efficiency and pollution			[42]

4. Results and Discussion

This section presents an evaluation of the outcome demonstrated by the three control strategies. MATLAB/Simulink has been used to implement the designed control system. The system parameters are detailed in Table 2, alongside the battery pack and SC parameters that have been studied in the previous section. The simulation profiles are derived from three distinct driving cycles, encompassing three unique environmental driving conditions to effectively test the controller performance of the optimised HESS.

The selected driving cycles are the Artemis rural cycle, the Artemis motorway with a speed differential of 150 km/h, and US06. These driving cycles are depicted in Figure 8. The Artemis rural cycle is designed to replicate driving conditions commonly found in rural areas, which are distinguished by reduced speeds and frequent stops and starts. This simulation accurately represents the stop-and-go aspect of country roadways. The motorway cycle represents high-speed motorway driving conditions, simulating sustained speeds of 150 km/h, typical of highway travel. Finally, the US06 cycle is a representation of rough driving circumstances, with its fast acceleration and deceleration patterns, which are

typical of city driving in heavy traffic. The attributes of each driving cycle are detailed in Table 4 [43]. The next section presents a more comprehensive examination of the efficiency and effectiveness of HESSs in optimising battery SOC across various driving cycles, utilising the insight obtained from the controller analysis.

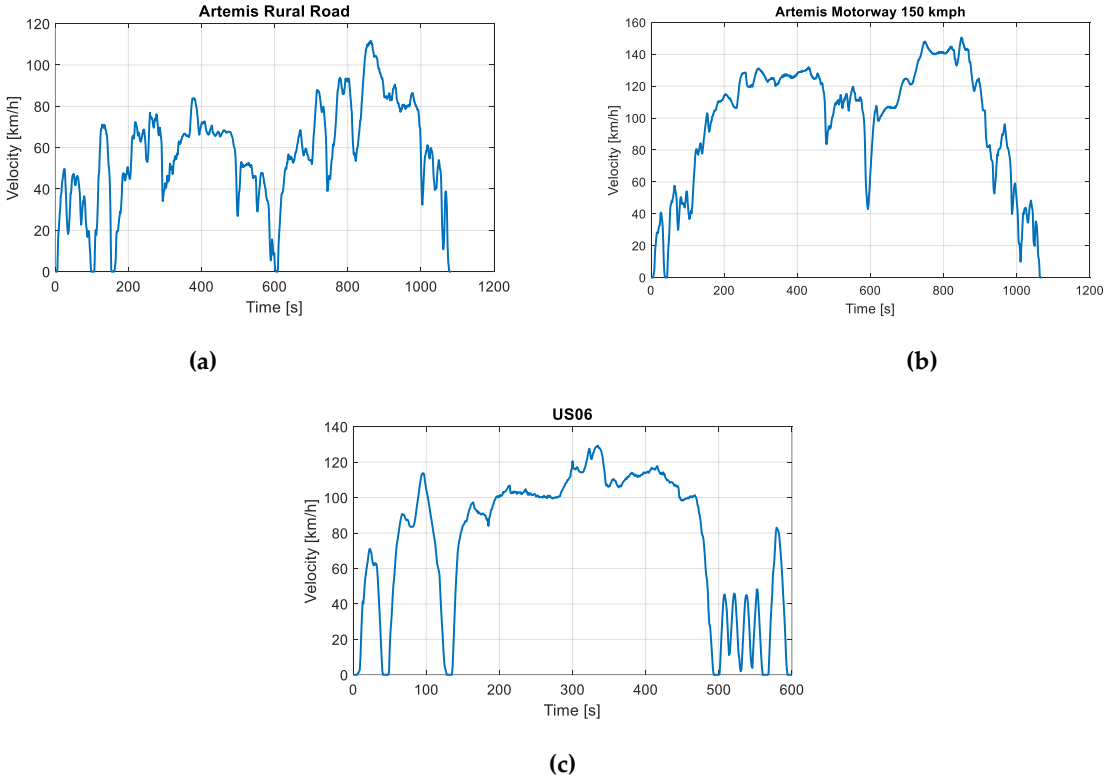

Figure 8. Representation of selected driving cycles: (**a**) Artemis rural, (**b**) Artemis motorway, (**c**) US06.

Table 4. Characteristics of each driving cycle [43].

Driving Cycle	Artemis Rural	Artemis 150 km/h Motorway	US06
Average Speed (km/h)	70	150	34.2
Type	Rural Roads	High-Speed Motorway	Aggressive Urban
Stops and Starts	Frequent	Few	Frequent
Acceleration Patterns	Varied	Sustained	Rapid
Speed Variability	Moderate	Minimal	High
Duration (s)	1082	1068	596
Traffic Condition	Light	Smooth	Heavy

4.1. Impact of HESSs on Battery Performance

The implementation of the HESS resulted in significant advancements in the management of battery SOC throughout all driving cycles that were examined. For this study, the analysis will focus on the initial 600 s for both Artemis driving cycle scenarios and the first 300 s of the US06 cycle. This deliberate selection aims to provide a clear and easily interpretable presentation of results. The choice to give priority to the first 600 s of the Artemis driving cycle scenarios and the first 300 s of the US06 cycle was made after careful consideration. This decision has been made to capture crucial times in battery performance during dynamic and demanding driving phases. For a detailed explanation of the time setup, refer to Section 4.2.

This approach was utilised to guarantee a thorough comprehension of battery SOC management, specifically in challenging start-up situations marked by significant interactions between energy demand and supply. The goal of this study aimed to enable a concentrated investigation by focusing on these particular periods, to provide useful insights that could be directly used in real-world situations. Ultimately, this approach aims to drive innovation and optimisation in battery technology for vehicle systems. The control system accurately determines the SOC of the battery by utilising real-time data from the battery management system. This system analyses variables such as voltage, current, and other relevant factors to provide an accurate estimation of the SOC.

Upon analysis of the Artemis rural cycle, it can be observed from Figure 9 that the introduction of the HESS led to a very consistent battery SOC profile for all three controllers, notably PI, MPC, and RBF. The stability of the HESS demonstrates its capacity to efficiently manage the balance between energy storage and distribution, hence reducing changes in SOC that may result in losses and rapid deterioration. The enhancement can be attributed to the HESS's capacity to utilise the high power density of SCs in managing abrupt power demands and transient loads. This decreases the strain on the battery, as it is more suitable for providing a consistent energy supply due to its higher energy density but lower power density. HESSs optimise the longevity and performance of the battery by dividing the load between the battery and supercapacitor, reducing the rate and depth of battery discharges. In addition, the HESS can effectively capture the energy from regenerative braking by utilising the SC, which can quickly charge and discharge. This process helps maintain the battery's SOC and enhances the overall energy efficiency.

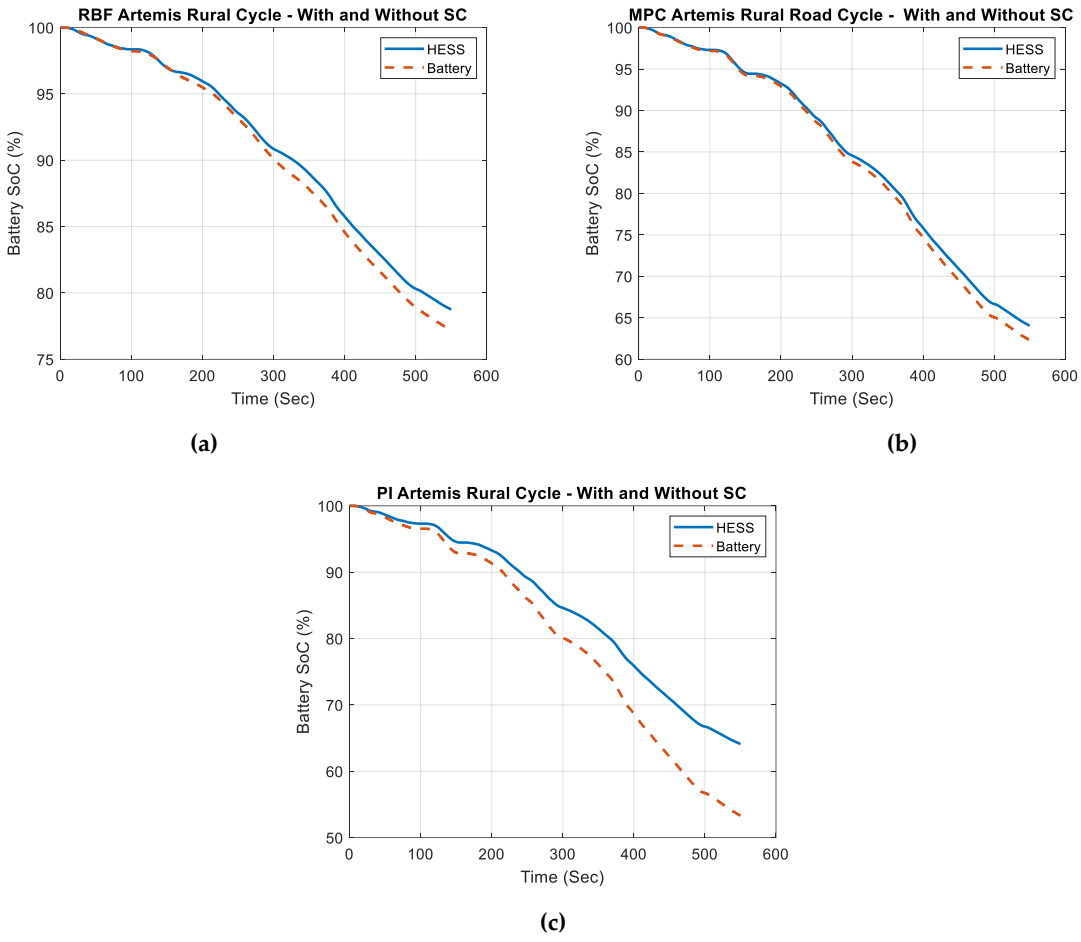

Figure 9. Battery SOC comparison over time for an HESS versus a standalone battery across various control strategies for the Artemis rural cycle. (**a**) SOC decay under the RBF, (**b**) SOC decay under the MPC, (**c**) SOC decay under the PI.

The same principle applies to the Artemis motorway cycle; the benefits of HESS integration persisted. This is evident from Figure 10, where all three controllers exhibited enhanced battery SOC control, with the HESS, ensuring a consistent and optimised SOC profile throughout the cycle. This consistency is crucial for EVs operating in high-speed conditions, where rapid energy fluctuations can occur.

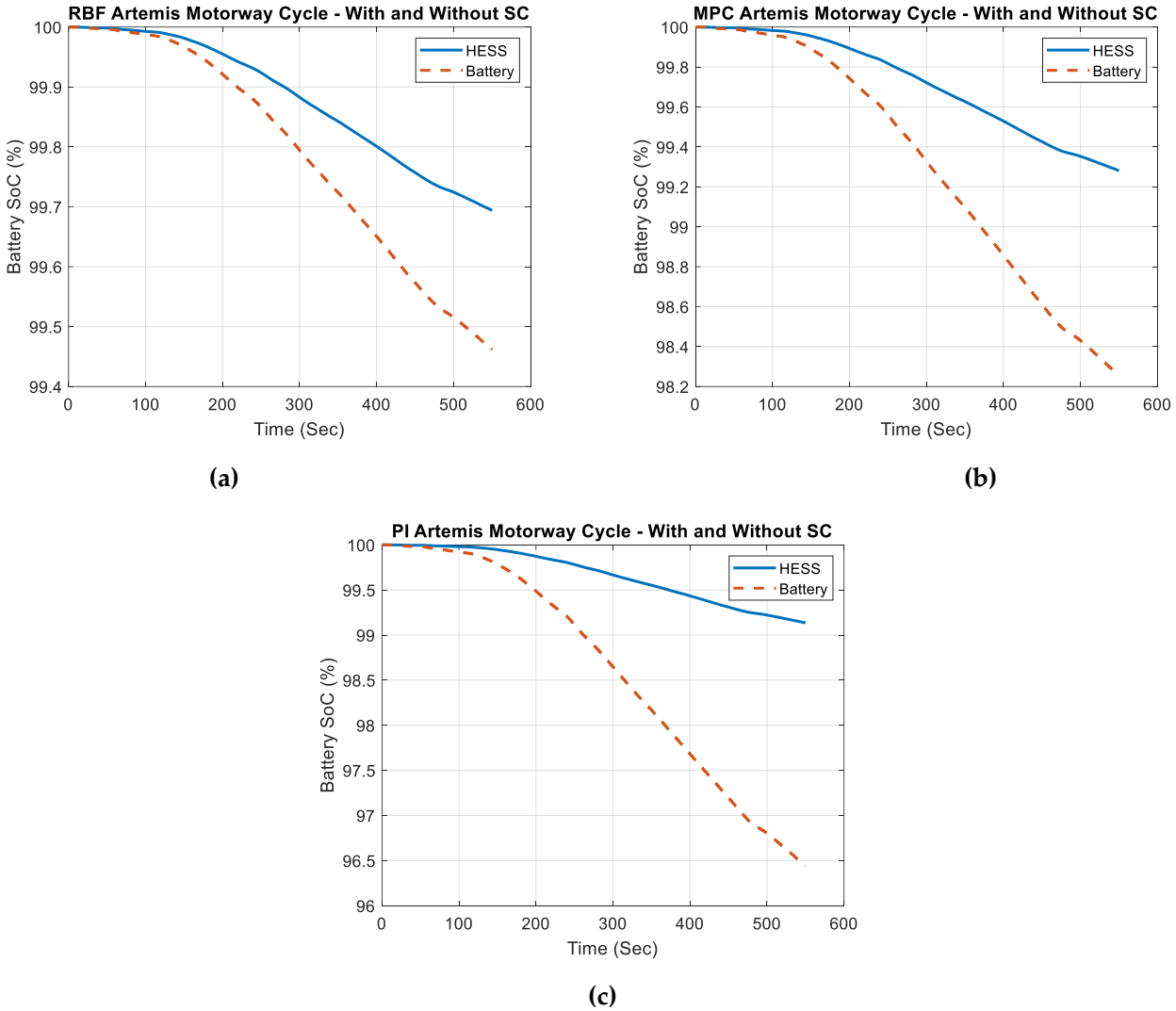

Figure 10. Battery SOC comparison over time for an HESS versus a standalone battery across various control strategies for the Artemis motorway cycle. (**a**) SOC decay under the RBF, (**b**) SOC decay under the MPC, (**c**) SOC decay under the PI.

Regarding the US06 cycle, the stability and effective management of the battery SOC were seen in all three controllers, as depicted in Figure 11. This demonstrates the adaptability of the HESS in handling dynamic and unpredictable driving situations. The capacity to adapt is crucial for practical EV applications, as different driving circumstances can significantly affect the storage and usage of energy.

The analysis of SOC across three distinct driving cycles provides valuable insights into the performance of various controllers in efficiently controlling the use of energy. In the context of the Artemis rural scenario, as depicted in Table 5, it is evident that the RBF regulator exhibits a higher efficiency in comparison to both the MPC and PI controllers, regardless of whether the system is battery only or an HESS. This is evident from the notably improved SOC values attained using the RBF controller, which signifies a reduced

energy usage. Conversely, the MPC and PI controllers exhibit lower SOC values, with the MPC controller substantially surpassing the PI controller.

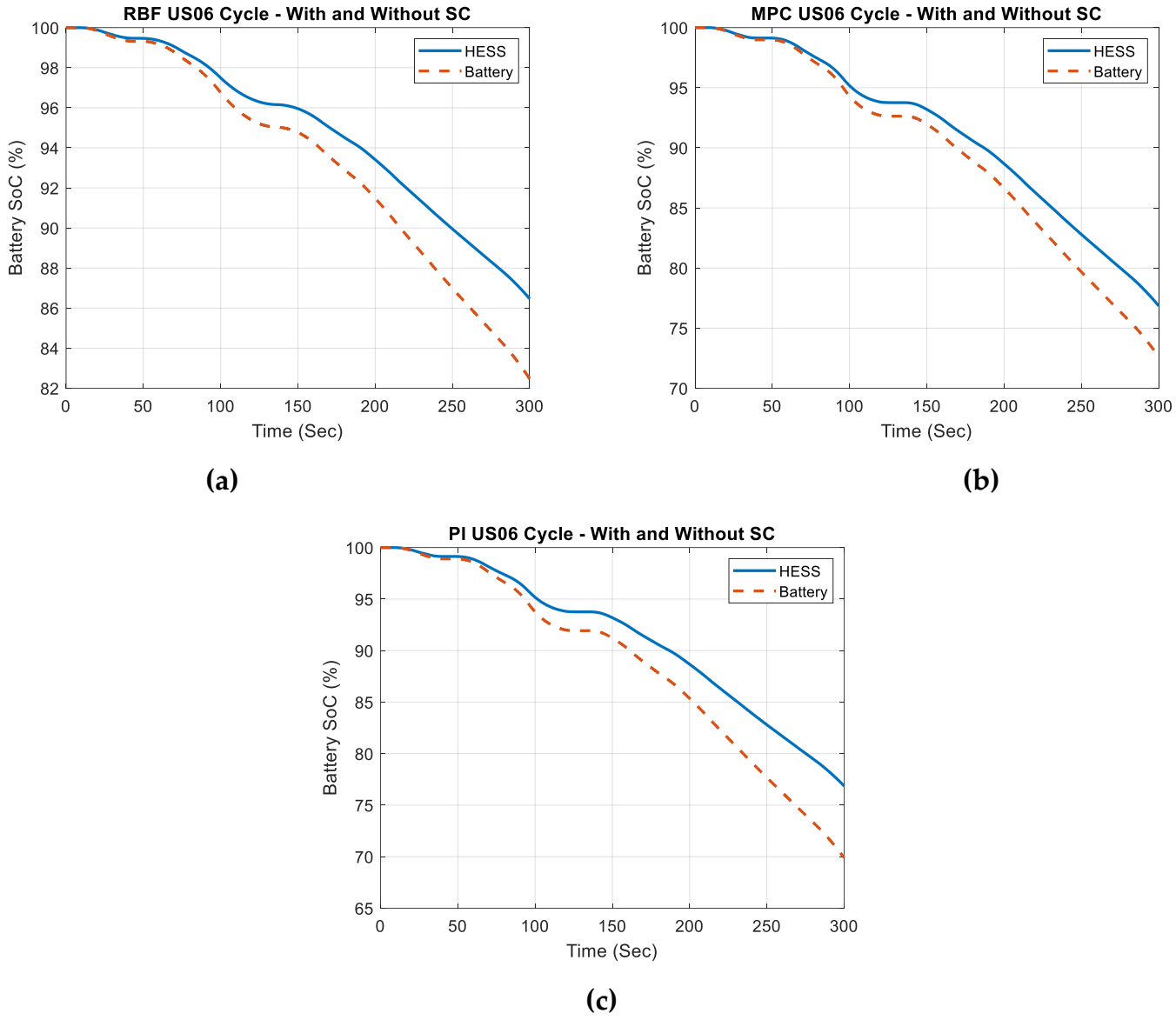

Figure 11. Battery SOC comparison over time for an HESS versus a standalone battery across various control strategies for US06. (**a**) SOC decay under the RBF, (**b**) SOC decay under the MPC, (**c**) SOC decay under the PI.

Table 5. Comparison of battery SOC for Artemis Rural.

	RBF	**MPC**	**PI**	**Energy Saved (kWh)**	
				RBF_PI	MPC_PI
Battery only	77.27%	62.5%	53.49%	5.66	2.11
HESS	78.86%	64.41%	64.2%	3.452	0.05

In the Artemis Motorway scenario depicted in Table 6, it can be observed that all controllers exhibit high SOC values, with just slight variations among them. Nevertheless, it is worth noting that the RBF controller exhibits an exceptional energy efficiency, particularly in the battery-only setup, thus demonstrating its efficacy in optimising energy utilisation.

Table 6. Comparison of battery SOC for Artemis Motorway.

	RBF	MPC	PI	Energy Saved (kWh)	
				RBF_PI	MPC_PI
Battery Only	99.47%	98.26%	96.47%	0.54	0.39
HESS	99.69%	99.28%	99.14%	0.11	0.04

The driving cycle of the US06, as depicted in Table 7, displays similar trends, with the RBF controller exhibiting the highest SOC, followed by the MPC and PI controllers. In summary, the findings reveal that the RBF controller effectively conserves energy in various driving conditions, making it a suitable choice for enhancing the efficiency of battery and HESSs. The distinctive urban driving characteristics of the US06 cycle, such as numerous starts and stops, quick acceleration, and significant speed variability, can be considered as the main reason for this. The RBF controller is particularly adept at meeting the requirements of these situations, which necessitate a highly sensitive energy management system. When comparing them, the Artemis rural and motorway cycles exhibit more consistent and stable driving patterns, leading to comparatively smaller improvements in SOC. The battery system is not as dynamically challenged by the frequent stops and starts at lower speeds of the rural cycle and the persistent high-speed driving of the motorway cycle, compared to the US06 cycle. Consequently, the US06 cycle exhibits a greater increase in the SOC as a result of the efficient utilisation of regenerative braking and the advanced control techniques offered by the RBF controller, which enhance energy efficiency in these challenging driving situations.

Table 7. Comparison of battery SOC for US06.

	RBF	MPC	PI	Energy Saved (kWh)	
				RBF_PI	MPC_PI
Battery Only	82.91%	72.75%	70.2%	3.09	0.61
HESS	86.46%	77.1%	77.1%	2.67	0

4.2. Impact of HESSs on SC Performance

Expanding on battery SOC, this subsection examines the influence of SCs on HESSs. By assessing the effect of HESSs on SC performance, significant findings emerge on the combined benefits that arise from including SCs as an additional energy source alongside batteries for EVs. The incorporation of SCs alongside EV batteries proves crucial for optimising the overall efficiency of the system. In the context of driving scenarios, the SC can play a role in supplementing power during acceleration, hence enhancing responsiveness and allowing a smoother driving interface. The SC's rapid charge and discharge attributes facilitate the provision of swift power bursts as required, particularly in situations requiring rapid acceleration or climbing a hill. The enhanced responsiveness of the vehicle benefits to its overall performance, yet preserves efficiency.

The examination of the SOC profiles of the SC under the influence of three controllers during each drive cycle, in conjunction with their corresponding SC charge and discharge profiles, offers valuable understanding surrounding the performance of each controller.

Throughout the Artemis rural driving cycle, the RBF controller regularly demonstrated superior efficiency by regularly achieving a higher SOC. The superior performance of the controller in terms of SOC improvements proved particularly apparent throughout the time intervals of 120–300 s, 380 s, and 500 s, as illustrated in Figure 12a. Furthermore, the power profiles for charging and discharging demonstrated the RBF controller's superiority, particularly evident within the initial 200 s. The charging/discharging profiles for the three controllers demonstrate the rapid adaptability to power requirements and the effective utilisation of regenerative energy, both of which play a vital role in the acceleration and

deceleration of EVs. Figure 12b provides further details on these features. Compared to the battery charging/discharging profile depicted in Figure 12c, the RBF controller demonstrates its dynamic and adaptive reaction to changing circumstances, as evidenced by its frequent and substantial fluctuations in power output. This behaviour demonstrates a control system that is very sensitive and capable of efficiently managing intricate and quickly evolving situations with accuracy. While MPC and PI controllers offer smoother responses, the RBF's agility is advantageous in applications that prioritise flexibility and rapid modifications.

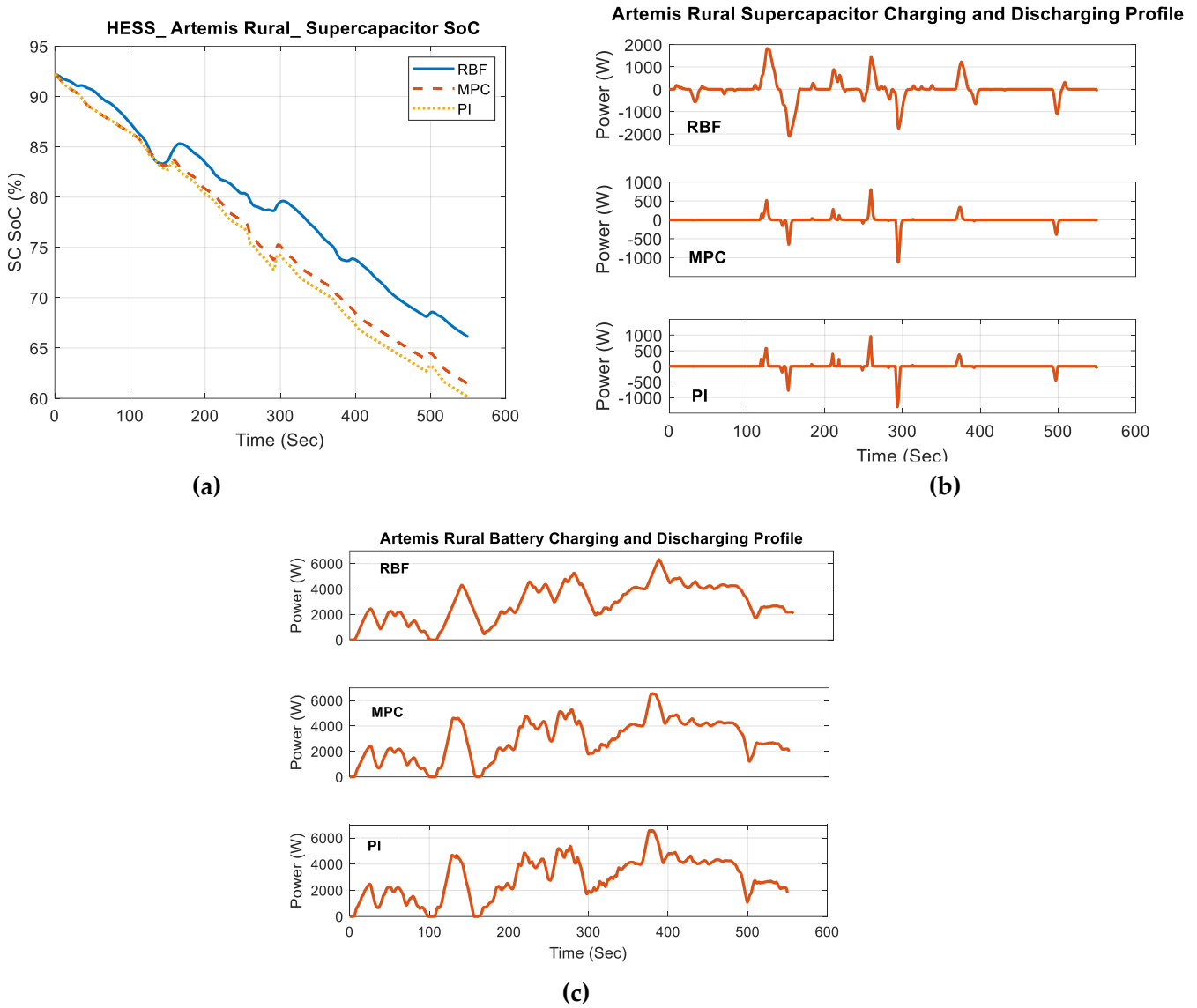

Figure 12. Artemis Rural: (**a**) SOC of SC, (**b**) charging/discharging profile of SC, (**c**) charging/discharging profile of battery.

The RBF controller proved exceptional proficiency in managing the SC charge during the Artemis highway cycle study, as demonstrated in Figure 13a. Although the RBF controller initially had a lower SOC, it demonstrated significant efficiency improvements, especially obvious between the 300 s and 500 s time intervals. In contrast, the PI controller exhibited a steady decline in the SOC, as depicted in Figure 13a. The charging and discharging patterns shown in Figure 13b exhibited a strong indication of the superior performance of the RBF controller, highlighting its capacity for efficiently controlling the energy flow of the SC. Being able to maintain consistent speeds is particularly crucial in the environment

of driving on motorways. The effective control of the RBF regulator assures excellent power availability and durability, thus being vital for longer high-speed journeys, even in steady-speed circumstances. Compared to the battery charging/discharging profile depicted in Figure 13c. The RBF controller demonstrates a highly steady and constant power output, maintaining a level very close to its maximum capacity during the entire time. The stability seen indicates a notable degree of accuracy and dependability in adapting to different circumstances, which is particularly important in situations that require a consistent and reliable performance. Conversely, the MPC exhibits a stable output, albeit with a bit more variability than the RBF method. This suggests that the MPC provides effective control, albeit with slightly less consistency. The PI controller, although effective, exhibits greater oscillations, indicating that it may be less appropriate for situations where power stability is of greatest significance.

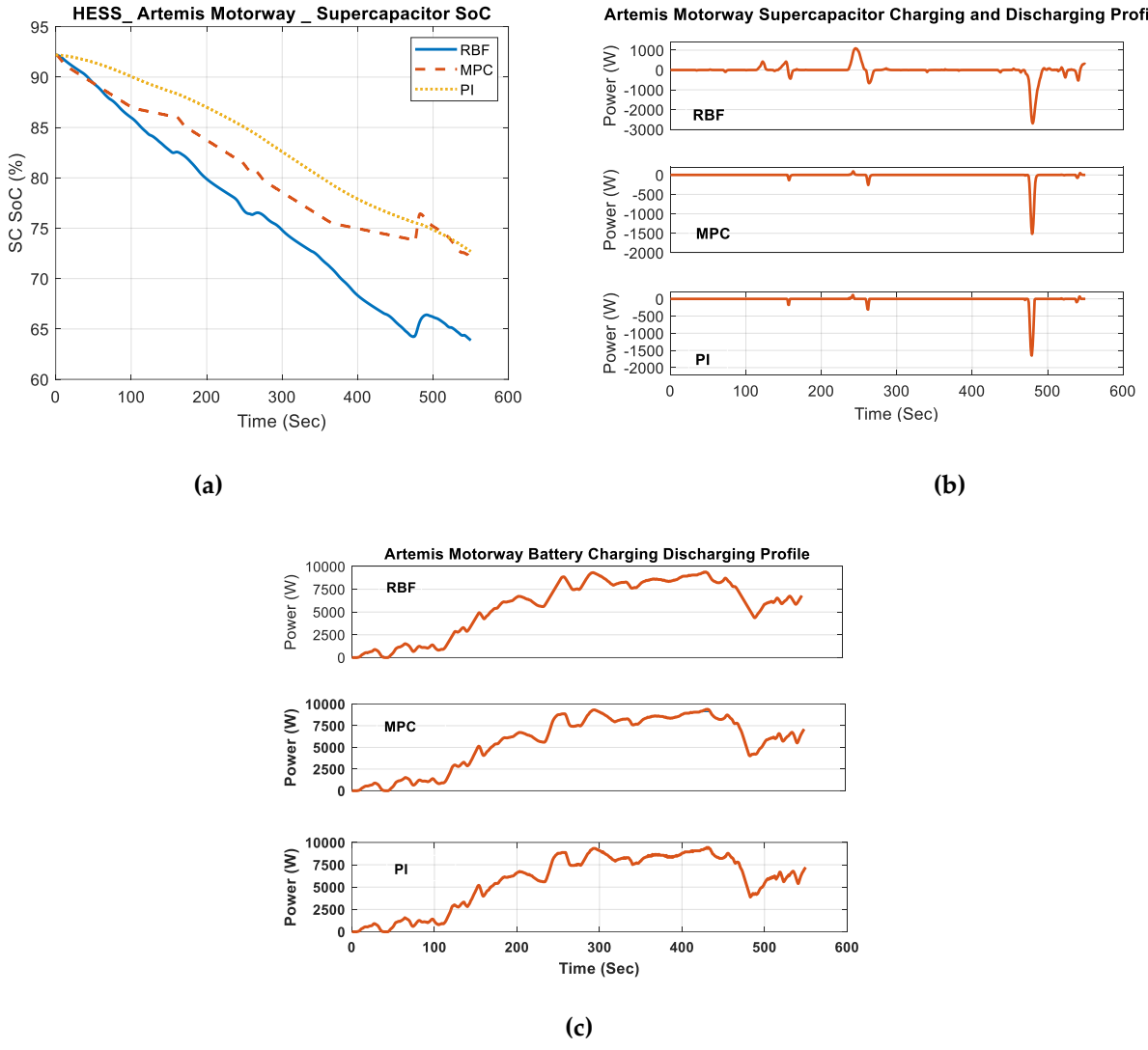

Figure 13. Artemis motorway: (**a**) SOC of SC, (**b**) charging/discharging profile of SC, (**c**) charging/discharging profile of battery.

In the analysis of the US06 cycle, it appeared that the RBF controller demonstrated a slightly lower SOC when compared to the MPC and PI controllers. However, it demonstrated an improvement within the 100 s time frame, as illustrated in Figure 14a. During the cycle, the energy profile indicated the RBF controller's capability to rapidly respond to variations in power, a crucial aspect in effectively handling the demanding acceleration and deceleration situations commonly observed in the US06 cycle. This can be observed in Figure 14b. Overall, the RBF controller consistently eclipsed the MPC and PI controllers in all cycles, demonstrating its superior energy management abilities. This results in greater assistance for EV acceleration, along with the effective utilisation of regenerative braking energy, which is crucial for extending battery life, as well as the effectiveness of electric vehicles. Compared to the battery charging/discharging profile depicted in Figure 14c, the RBF controller exhibits a greater level of stability and maintains a consistently high power output over the entire duration, especially following the early fluctuations. This demonstrates a greater capacity to handle disruptions and adjust to fluctuating circumstances, emphasising its strength and effectiveness in maintaining target power levels. The RBF exhibits less instability and a more consistent power output profile compared to MPC and PI, making it an ideal option for EV applications that need great dependability and precision.

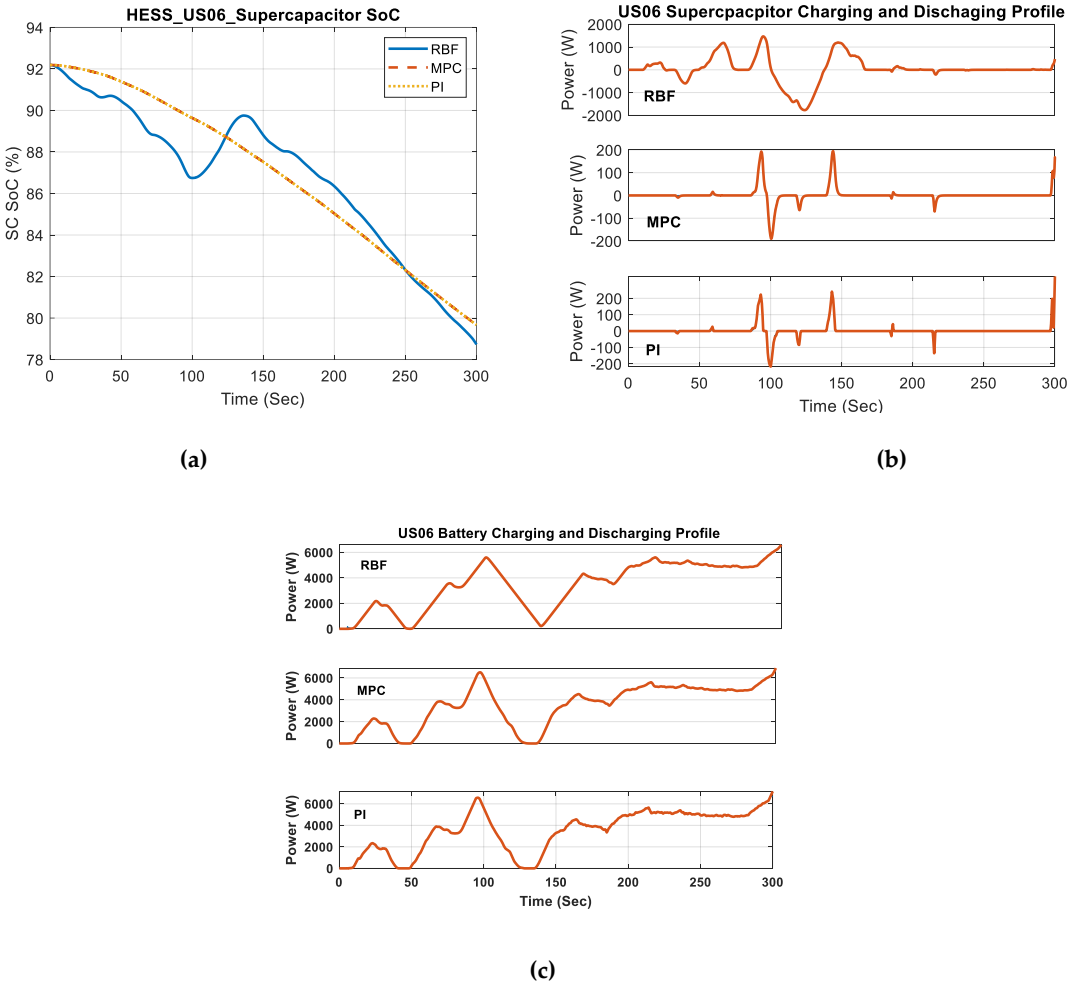

Figure 14. US06: (**a**) SOC of SC, (**b**) charging/discharging profile of SC, (**c**) charging/discharging profile of battery.

4.3. Overall System Efficiency and Performance

By combining HESSs with EVs, as demonstrated using the Artemis rural, Artemis motorway, and US06 driving cycles, there is a substantial improvement in the management of battery SOC and the efficiency of SCs. When the HESS is exposed to different driving scenarios, such as situations that need high power, quick acceleration, and fluctuating speeds, it shows an improved responsiveness and energy management. During periods of high acceleration, the SC delivers rapid surges of power, reducing the burden on the battery and keeping the SOC steady. This effect is most noticeable in the US06 cycle. Artemis rural cycles effectively handle frequent stops and starts by optimising energy demand distribution between the battery and SC, resulting in minimised energy losses and battery degradation. During constant high speeds on the motorway cycle, the HESS ensures a steady SOC, which is crucial for long-duration travel. This study primarily examines the Nissan Leaf; however, the control strategies described can be tailored for other EV models by adjusting control parameters to align with their unique attributes. This guarantees that the advantages of HESSs, including enhanced SOC management along with improved SC performance, can be achieved in different EVs. In summary, the integration of HESSs improves energy management, improves vehicle performance, and extends the lifespan of the battery. This underscores the significance of employing advanced control algorithms for sustainable transportation.

5. Conclusions

The assessment of a fully active HESS in a Nissan Leaf has shown substantial improvements in energy management and dependability in different driving situations. The study validates that integrating SCs with batteries in a HESS not only helps to manage the SOC of the battery, but also enhances the system's overall energy efficiency compared to conventional battery-only systems. The RBF controller consistently outperformed traditional controllers in dynamic and unexpected environments, thus validating its appropriateness for real-world applications in EVs. It is worth mentioning that although the Artemis highway and US06 cycles show significant enhancements, the rural cycle posed difficulties in sustaining an appropriate SOC. This indicates that the technique may need additional adjustments for situations including frequent stops and low speeds.

The findings highlight the significance of utilising advanced control algorithms in HESSs to improve electric vehicles' efficiency and long-term durability. This will aid in their greater feasibility and sustainability in tackling global energy challenges. This research not only strengthens current knowledge by presenting actual evidence of the effectiveness of different control systems in HESSs, but also creates opportunities for further study. Further research should explore the incorporation of adaptive learning models that can flexibly adapt to various driving behaviours and environmental fluctuations. Furthermore, conducting further studies to investigate the efficacy of HESSs in large-scale vehicles and areas with severe atmospheric conditions will result in a full comprehension of its practical uses and restraints.

This study lays the foundation for progress in EV technology and energy management methods, fostering the creation of tailored control systems that can be adjusted to different driving circumstances.

Author Contributions: Conceptualization, M.F., C.S.L. and M.D.; methodology, M.F. and C.S.L.; software, M.F.; validation, M.F.; formal analysis, M.F.; investigation, M.F.; resources, C.S.L. and G.T.; data curation, M.F.; writing—original draft preparation, M.F, C.S.L. and M.D.; writing—review and editing, G.T.; supervision, C.S.L. and M.D.; All authors have read and agreed to the published version of the manuscript.

Funding: This research is funded by the National Natural Science Foundation of China (62206062) and the EPSRC Doctoral Training Programme.

Data Availability Statement: The data that support the findings of this study are available from the corresponding authors upon reasonable request.

Conflicts of Interest: The authors declare no conflicts of interest.

References

1. Smit, R.; Whitehead, J.; Washington, S. Where are we heading with electric vehicles? *Air Qual. Clim. Change* **2018**, *52*, 18–27.
2. Sanguesa, J.A.; Torres-Sanz, V.; Garrido, P.; Martinez, F.J.; Marquez-Barja, J.M. A Review on Electric Vehicles: Technologies and Challenges. *Smart Cities* **2021**, *4*, 372–404. [CrossRef]
3. Üçok, M. Prospects for hydrogen fuel cell vehicles to decarbonize road transport. *Discov. Sustain.* **2023**, *4*, 42. [CrossRef]
4. Yong, T.; Park, C. A qualitative comparative analysis on factors affecting the deployment of electric vehicles. *Energy Procedia* **2017**, *128*, 497–503. [CrossRef]
5. Rimpas, D.; Kaminaris, S.D.; Aldarraji, I.; Piromalis, D.; Vokas, G.; Papageorgas, P.G.; Tsaramirsis, G. Energy management and storage systems on electric vehicles: A comprehensive review. *Mater. Today Proc.* **2022**, *61*, 813–819. [CrossRef]
6. Traoré, B.; Doumiati, M.; Morel, C.; Olivier, J.-C.; Soumaoro, O. Energy management strategy design based on frequency separation, fuzzy logic and Lyapunov control for multi-sources electric vehicles. In Proceedings of the IECON 2019-45th Annual Conference of the IEEE Industrial Electronics Society, Lisbon, Portugal, 14–17 October 2019; IEEE: Piscataway, NJ, USA, 2019; pp. 2676–2681.
7. Ju, F.; Zhang, Q.; Deng, W.; Li, J. Review of structures and control of battery-supercapacitor hybrid energy storage system for electric vehicles. In *Advances in Battery Manufacturing, Service, and Management Systems*; Wiley-IEEE Press: Piscataway, NJ, USA, 2016; pp. 303–318.
8. Xiang, C.; Wang, Y.; Hu, S.; Wang, W. A New Topology and Control Strategy for a Hybrid Battery-Ultracapacitor Energy Storage System. *Energies* **2014**, *7*, 2874–2896. [CrossRef]
9. Tie, S.; Tan, C.W. A review of energy sources and energy management system in electric vehicles. *Renew. Sustain. Energy Rev.* **2013**, *20*, 82–102. [CrossRef]
10. Cao, J.; Emadi, A. A New Battery/UltraCapacitor Hybrid Energy Storage System for Electric, Hybrid, and Plug-In Hybrid Electric Vehicles. *IEEE Trans. Power Electron.* **2012**, *27*, 122–132. [CrossRef]
11. Farrag, M.; Lai, C.S.; Darwish, M. Overview of Electric Vehicle Interconnected Subsystems. In Proceedings of the 2022 57th International Universities Power Engineering Conference (UPEC), Istanbul, Turkey, 30 August–2 September 2022; pp. 1–6. [CrossRef]
12. Dhifli, M.; Jawadi, S.; Lashab, A.; Guerrero, J.M.; Cherif, A. An efficient external energy maximization-based energy management strategy for a battery/supercapacitor of a micro grid system. *Int. J. Comput. Sci. Netw. Secur.* **2020**, *20*, 196–203.
13. Veneri, O.; Capasso, C.; Patalano, S. Experimental investigation into the effectiveness of a super-capacitor based hybrid energy storage system for urban commercial vehicles. *Appl. Energy* **2018**, *227*, 312–323. [CrossRef]
14. Bharath, K.V.S.; Pandey, K. Fuzzy-based multi-objective optimization for subjection and diagnosis of hybrid energy storage system of an electric vehicle. In *Proceeding of International Conference on Intelligent Communication, Control and Devices (ICICCD 2016)*; Springer: Berlin/Heidelberg, Germany, 2017; pp. 299–307. ISBN 9811017077.
15. Sellali, M.; Abdeddaim, S.; Betka, A.; Djerdir, A.; Drid, S.; Tiar, M. Fuzzy-Super twisting control implementation of battery/super capacitor for electric vehicles. *ISA Trans.* **2019**, *95*, 243–253. [CrossRef] [PubMed]
16. Zhang, X.; Lu, Z.; Lu, M. Vehicle speed optimized fuzzy energy management for hybrid energy storage system in electric vehicles. *Complexity* **2020**, *2020*, 2073901. [CrossRef]

17. Zhang, Q.; Deng, W.; Li, G. Stochastic control of predictive power management for battery/supercapacitor hybrid energy storage systems of electric vehicles. *IEEE Trans. Industr. Inform.* **2017**, *14*, 3023–3030. [CrossRef]
18. Wu, Y.; Huang, Z.; Liao, H.; Chen, B.; Zhang, X.; Zhou, Y.; Liu, Y.; Li, H.; Peng, J. Adaptive power allocation using artificial potential field with compensator for hybrid energy storage systems in electric vehicles. *Appl. Energy* **2020**, *257*, 113983. [CrossRef]
19. Sun, L.; Feng, K.; Chapman, C.; Zhang, N. An Adaptive Power Split Strategy for Battery-Supercapacitor Powertrain–Design, Simulation and Experiment. *IEEE Trans. Power Electron.* **2017**, *32*, 9364–9375. [CrossRef]
20. Song, Z.; Hofmann, H.; Li, J.; Han, X.; Ouyang, M. Optimization for a hybrid energy storage system in electric vehicles using dynamic programing approach. *Appl. Energy* **2015**, *139*, 151–162. [CrossRef]
21. Zhang, S.; Xiong, R.; Cao, J. Battery durability and longevity based power management for plug-in hybrid electric vehicle with hybrid energy storage system. *Appl. Energy* **2016**, *179*, 316–328. [CrossRef]
22. Shen, J.; Khaligh, A. A Supervisory Energy Management Control Strategy in a Battery/Ultracapacitor Hybrid Energy Storage System. *IEEE Trans. Transp. Electrif.* **2015**, *1*, 1. [CrossRef]
23. Li, M.; Wang, L.; Wang, Y.; Chen, Z. Sizing Optimization and Energy Management Strategy for Hybrid Energy Storage System Using Multi-objective Optimization and Random Forests. *IEEE Trans. Power Electron.* **2021**, *36*, 11421–11430. [CrossRef]
24. Wang, L.; Li, M.; Wang, Y.; Chen, Z. Energy Management Strategy and Optimal Sizing for Hybrid Energy Storage Systems Using an Evolutionary Algorithm. *IEEE Trans. Intell. Transp. Syst.* **2022**, *23*, 24183–24193. [CrossRef]
25. Pérez, V.H.; Gaztañaga, H.; Milo, A.; Saez-de-Ibarra, A.; Etxeberria-Otadui, I.; Nieva, T. Optimal Energy Management and Sizing of a Battery Supercapacitor based Light Rail Vehicle with Multi-objective approach. *IEEE Trans. Ind. Appl.* **2016**, *52*, 3367–3377.
26. Xu, D.; Cui, Y.; Ye, J.; Cha, S.W.; Li, A.; Zheng, C. A soft actor-critic-based energy management strategy for electric vehicles with hybrid energy storage systems. *J. Power Sources* **2022**, *524*, 231099. [CrossRef]
27. Li, F.; Gao, Y.; Wu, Y.; Xia, Y.; Wang, C.; Hu, J.; Huang, Z. Incentive learning-based energy management for hybrid energy storage system in electric vehicles. *Energy Convers. Manag.* **2023**, *293*, 117480. [CrossRef]
28. Wu, Y.; Huang, Z.; Zheng, Y.; Liu, Y.; Li, H.; Che, Y.; Peng, J.; Teodorescu, R. Spatial–temporal data-driven full driving cycle prediction for optimal energy management of battery/supercapacitor electric vehicles. *Energy Convers. Manag.* **2023**, *277*, 116619. [CrossRef]
29. Katnapally, A.; Manthati, U.B.; Raveendran, A.C.; Punna, S. A predictive power management scheme for hybrid energy storage system in electric vehicle. *Int. J. Circuit Theory Appl.* **2021**, *49*, 3864–3878. [CrossRef]
30. Chen, H.; Xiong, R.; Lin, C.; Shen, W. Model predictive control based real-time energy management for hybrid energy storage system. *CSEE J. Power Energy Syst.* **2020**, *7*, 862–874.
31. Gharibeh, H.F.; Khiavi, L.M.; Farrokhifar, M.; Alahyari, A.; Pozo, D. Power Management of Electric Vehicle Equipped with Battery and Supercapacitor Considering Irregular Terrain. In Proceedings of the 2019 International Youth Conference on Radio Electronics, Electrical and Power Engineering (REEPE), Moscow, Russia, 14–15 March 2019; pp. 1–5. [CrossRef]
32. Zhang, Q.; Ju, F.; Zhang, S.; Deng, W.; Wu, J.; Gao, C. Power Management for Hybrid Energy Storage System of Electric Vehicles Considering Inaccurate Terrain Information. *IEEE Trans. Autom. Sci. Eng.* **2017**, *14*, 608–618. [CrossRef]
33. Argonne National Laboratory. Electric Vehicle TestingPublic. Available online: https://www.anl.gov/taps/electric-vehicle-testing (accessed on 2 May 2024).
34. Baboselac, I.; Hederić, Ž.; Bensic, T. MatLab simulation model for dynamic mode of the Lithium-Ion batteries to power the EV. *Tech. J.* **2017**, *11*, 7–13.
35. Katuri, R.; Gorantla, S. Design and simulation of a controller for a hybrid energy storage system based electric vehicle. *Math. Model. Eng. Probl.* **2019**, *6*, 203–216. [CrossRef]
36. Mobariz, K.; Mobarez, E.; Ashry, M. Fuel Cell Propulsion Control System Based On PID Approaches. In Proceedings of the 2021 17th International Computer Engineering Conference (ICENCO), Cairo, Egypt, 29–30 December 2021. [CrossRef]
37. Kumar, M.; Sen, S.; Prajapati, A.K.; Diwania, S. A Comprehensive Power Management Approach for Hydrogen Fuel-cell-Based Hybrid EVs Using PID Controller. In Proceedings of the 2023 IEEE IAS Global Conference on Renewable Energy and Hydrogen Technologies (GlobConHT), Male, Maldives, 11–12 March 2023; IEEE: Piscataway, NJ, USA, 2023; pp. 1–6.
38. Huang, W.; Lu, Z.; Cao, X.; Hou, Y. Hierarchical Coordinated Energy Management Strategy for Hybrid Energy Storage System in Electric Vehicles Considering the Battery's SOC. *Systems* **2023**, *11*, 498. [CrossRef]
39. Xin, W.; Xu, E.; Zheng, W.; Feng, H.; Qin, J. Optimal energy management of fuel cell hybrid electric vehicle based on model predictive control and on-line mass estimation. *Energy Rep.* **2022**, *8*, 4964–4974. [CrossRef]
40. Hao, J.; Ruan, S.; Wang, W. Model Predictive Control Based Energy Management Strategy of Series Hybrid Electric Vehicles Considering Driving Pattern Recognition. *Electronics* **2023**, *12*, 1418. [CrossRef]
41. Li, L.; Tao, F.; Fu, Z. Robust mode transition control of four-wheel-drive hybrid electric vehicles based on radial basis function neural network estimation-a simulation study. *COMPEL-Int. J. Comput. Math. Electr. Electron. Eng.* **2021**, *40*, 870–887. [CrossRef]

42. Harris, T. *Implementation of Radial Basis Function Artificial Neural Network into an Adaptive Equivalent Consumption Minimization Strategy for Optimized Control of a Hybrid Electric Vehicle*; West Virginia University: Morgantown, WV, USA, 2020. [CrossRef]
43. Barlow, T.; Latham, S.; McCrae, I.S.; Boulter, P. A Reference Book of Driving Cycles for Use in the Measurement of Road Vehicle Emissions. *TRL Published Project Report*. 2009. Available online: https://api.semanticscholar.org/CorpusID:106562433 (accessed on 27 April 2024).